



# Preparation and Characterization of $Gd_{1-x}Sr_xAlO_3$ Cathode for Solid Oxide Fuel Cell

M. Rajasekhar\*, N. Kalaivani

Department of chemistry, Government Arts College, Dharmapuri, TN, India

Received: 01.07.2017 Accepted: 11.07.2017 Published: 30-09-2017

\*drmrchem@gmail.com

## ABSTRACT

$Gd_{1-x}Sr_xAlO_3$  ( $0 \leq x \leq 0.5$ ) cathode materials are synthesized with  $Gd(NO_3)_3$ ,  $Sr(NO_3)_2$ ,  $Al(NO_3)_3$ , and aspartic acid (fuel) by combustion method with heating at  $550^\circ C$  for 6 hours. The surface morphology of the synthesized crystalline powder is characterized by Scanning Electron Microscopy (SEM). Thus, particle size and porosity were determined. The synthesis and crystallization are followed by thermochemical techniques (TGA/DTA). The synthesized materials show reasonable electrical conductivity. These results indicate that combustion method is a promising method to prepare nanocrystalline  $Gd_{1-x}Sr_xAlO_3$  for Intermediate Solid Oxide Fuel Cell.

**Keywords:** Ionic conductivity; Scanning Electron Microscopy; Transmission Electron Microscope; Thermal analysis.

## 1. INTRODUCTION

Fuel cells are electrochemical device that converts the chemical energy directly into electrical energy. The challenge is to develop material with good performance at intermediate temperature ( $500-800^\circ C$ ) for SOFCs allowing to reduce the cost of the cell and increasing the long-term stability. For the fuel cell, the most commonly used materials are lanthanum strontium manganite (LSM) was used for the cathode, YSZ for the electrolyte and Ni-YSZ cermet for the anode. It is essential that the chosen interconnect material have highest chemical stability, the highest oxidation resistance as well as the highest electrical conductivity.

The permanent increment of human population is accompanied by increase of energy demand and more restrictive environmental regulations. In that instance, the Solid Oxide Fuel Cells (SOFC) technology has emerged as an efficient substitution of the presently existing energy devices. Fuel cells are important type of electrochemical devices which converts chemical energy into electrical energy in a clean and calm way. Assisted combustion synthesis (ACS) or self-propagating high-temperature synthesis (SHS) is an effective, low-cost method for production of various industrially useful materials. They have wide range of potential applications ranging from providing power for portable devices (eg. Mobile phones, laptop computers) and transport applications to small and large scale stationary power applications.

The assisted combustion method is a novel method in the production of ultra-fine ceramic powders with a small particle size and high porosity. Fuel cells

have many advantages compared to conventional electric power generation systems such as high conversion efficiency which is relatively independent of size as well as environmental compatibility.

## 2. EXPERIMENTAL STUDIES

The nanocrystalline  $Gd_{1-x}Sr_xAlO_3$  powder was synthesized by assisted combustion method using high purity of  $Gd(NO_3)_3$ ,  $Sr(NO_3)_2$ ,  $Al(NO_3)_3$  and aspartic acid as fuel. All the reagents were purchased from Sigma Aldrich, (>99.9%), the required stoichiometric amounts of the starting materials were dissolved in double distilled deionized water in order to obtain a homogeneous solution. This solution was kept at constant heating at  $80^\circ C$  to obtain the foamy powders of  $Gd_{1-x}Sr_xAlO_3$  is shown in flow chart as 2.1. For Calcination, the foamy powder was carried out in a muffle furnace at  $550^\circ C$  for six hours.

## 3. CHARACTERIZATION ANALYSIS

X-ray powder diffraction (XRD) data were collected at room temperature with a diffractometer (Model: Philips X'Pert MPH<sup>R</sup>) with  $Cu K\alpha$  radiation. The data were recorded in the  $2\theta$  range of  $10-70^\circ$  with a  $0.02^\circ$  steps. The particle size and morphology of the produced powder was analysed with a JEOL scanning electron microscopy SEM (Model: JSM-840A) equipment with INCA was used to determine the morphology of samples.

The thermal decomposition of the polymeric precursors was characterized by Perkin-Elmer TG/DTA thermal analysis (Model: Pyris Diamond). The TGA is a process which relies on measuring the change in physical

and chemical properties of a sample as a function of temperature (with constant heating rate) or as a function of time (with constant temperature). It is predominantly used for determining the features of a material that exhibit either mass loss or gain due to decomposition, oxidation or loss of volatiles. Differential thermal analysis is a technique in which the temperature of a sample is compared with an inert reference material during the programmed change of temperature.

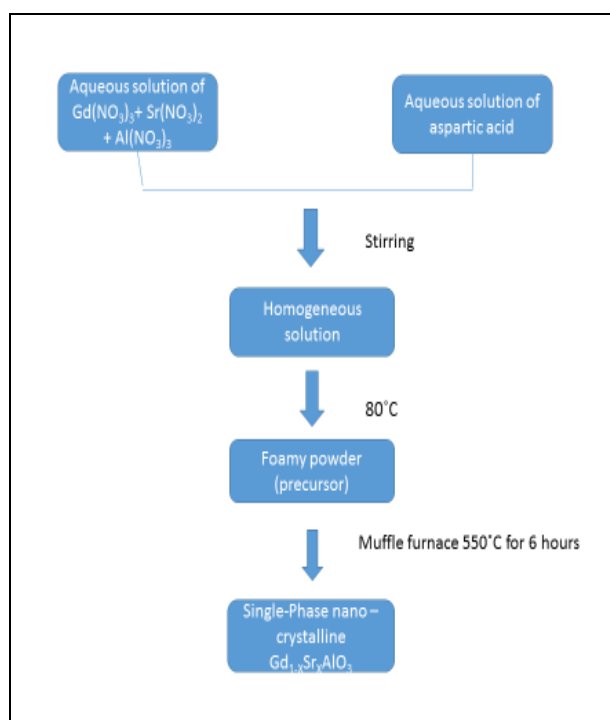


Fig. 1: Flow chart of assisted combustion synthesis of  $Gd_{1-x}Sr_xAlO_3$

The particle size of the synthesized powder was observed by means of a JOEL transmission electron microscopy (Model: 1200 EX). The synthesized powder was analysed with FTIR spectrometry. (Agilent Cary 630 FTIR spectrometer) and which scanned in a region of about  $4000-400\text{cm}^{-1}$ . The ionic conductivity of the sintered pellets were measured by a dc-four probe method which temperatures range  $200-700^\circ\text{C}$  in air.

## 4. RESULTS & DISCUSSION

### 4.1 Analysis of Crystalline Structure

The powder XRD analysis was performed on the prepared  $Gd_{1-x}Sr_xAlO_3$  nanocrystalline powders at  $550^\circ\text{C}$  for 6 hours. It was used identifying the crystallite size of  $Gd_{1-x}Sr_xAlO_3$  powder. The perovskite phase has existed in the resulting powder but the impurity phase has exist clearly as well. In general, all the diffracted peaks are broader than usually observed for highly crystalline powder. The broadening in the diffracted peaks is attributed to the superfine crystalline nature of

composites. The size of the particles were calculated by Scherrer equation, it was 30 nm.

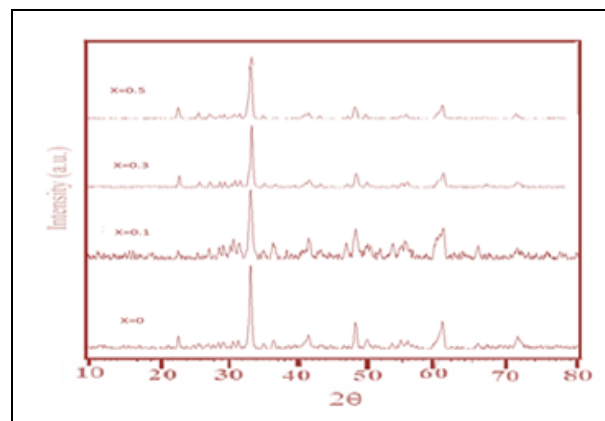


Fig. 2: X-ray diffraction pattern of  $Gd_{1-x}Sr_xAlO_3$

### 4.2 SEM Analysis

Fig. 3 shows the SEM microstructure of  $Gd_{0.7}Sr_{0.3}AlO_3$  powder obtained at  $550^\circ\text{C}$  for 6 hours. The surface morphology of the synthesized product is different pores and grains. Further, the SEM image indicates that the particles are agglomeration. All the samples are relatively dense and do not show much difference in density. However Sr doping significantly improves the grain growth. The average grain size of the doped samples is between 4 and  $12\ \mu\text{m}$ . The average crystallite size is 30 nm. The particles are uniformly distributed. There is agglomeration of the particles. The particles of the synthesized products are in nanorange.

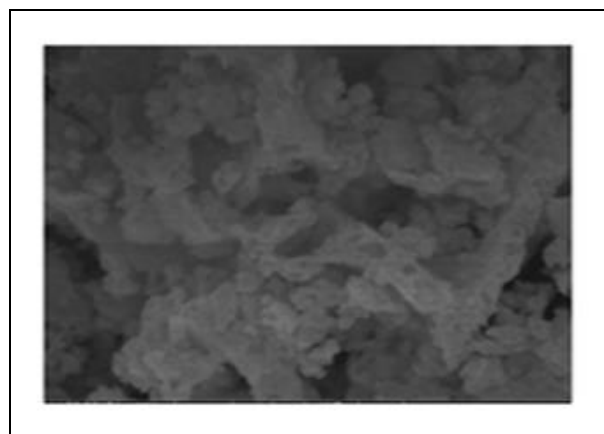


Fig. 3: SEM photograph of  $Gd_{0.7}Sr_{0.3}AlO_3$

### 4.3. Thermal Analysis of TGA/DTA

Fig. 4 shows that the TGA/DTA pattern obtained on  $Gd_{1-x}Sr_xAlO_3$  powder. The sample heating from  $100^\circ\text{C}$ - $800^\circ\text{C}$  which shows slight weight loss of about  $0.035\text{mg}/\text{min}$ . Again the sample shows a weight increase from  $105.3^\circ\text{C}$ - $386.39^\circ\text{C}$  of  $0.070\text{mg}/\text{min}$ . The weight gain and weight loss indicate the  $Gd_{0.7}Sr_{0.3}AlO_3$

powder exhibited easy reversible absorption-desorption of oxygen from air. The weight loss is minimum because of the removal of residual H<sub>2</sub>O and different gases. The chemical decomposition with increases of temperature was examined through DTA and it appeared as the endothermic and exothermic peaks. From the above TGA/DTA data, know the Gd<sub>0.7</sub>Sr<sub>0.3</sub>AlO<sub>3</sub> gradually absorbs the oxygen from air with temperature.

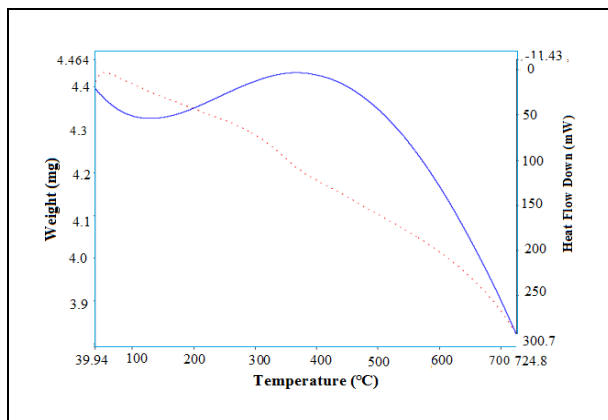


Fig. 4: TGA & DTA of Gd<sub>0.7</sub>Sr<sub>0.3</sub>AlO<sub>3</sub>

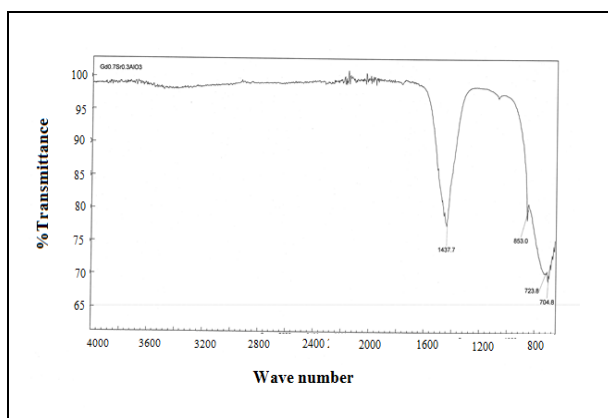


Fig. 5: FT-IR spectrum of Gd<sub>0.7</sub>Sr<sub>0.3</sub>AlO<sub>3</sub>

#### 4.4 FTIR Analysis

FTIR spectroscopy was used to confirm metal oxide bond formation in the crystal and is investigated their vibrational behavior in solid state of Gd<sub>1-x</sub>Sr<sub>x</sub>AlO<sub>3</sub> powder. It was recorded in the range of 4000 cm<sup>-1</sup> to 400 cm<sup>-1</sup>. The infrared spectrums of synthesized samples of Gd<sub>0.7</sub>Sr<sub>0.3</sub>AlO<sub>3</sub> powder are shown in fig. 5. The broad band at 1437.7 cm<sup>-1</sup> is assigned to vibration mode of chemically bonded hydroxyl groups. The peak appeared at 853.0 cm<sup>-1</sup> corresponds to the H-O-H bond mode confirming the presence of moisture in the sample. The peak appeared at 1437.7 cm<sup>-1</sup> is due to the presence of CO<sub>2</sub> in the sample. The Gd<sub>0.7</sub>Sr<sub>0.3</sub>AlO<sub>3</sub> exhibited a low intensity peak at 704.8 cm<sup>-1</sup> and the sample exhibited three peaks obtained between the wavelength regions 600-1000 cm<sup>-1</sup> which observed at 853.0, 723.8, and

704.8 cm<sup>-1</sup>. The peak appeared at 1437.7 cm<sup>-1</sup> is related to the O-H stretching vibration of H<sub>2</sub>O in the sample. The broad band at 1437.7 cm<sup>-1</sup> is assigned to vibration mode of chemically bonded hydroxyl groups.

#### 4.5 Conductivity

Fig. 6 shows that the Arrhenius plots of conductivity for Gd<sub>1-x</sub>Sr<sub>x</sub>AlO<sub>3</sub> samples sintered at different temperature range. It can be seen from Fig. 6, that the conductivity of the samples increases gradually with increasing the temperature. In this case, grains grow excessively, and the pores are trapped among the grains or grain boundaries, blocking oxygen ion migration leading to the decreases in the conductivity of the sample. The volatilization of gaseous SrO and O<sub>2</sub> from Gd<sub>1-x</sub>Sr<sub>x</sub>AlO<sub>3</sub> at excessively high sintering temperature were detected by mass spectroscopy resulting in the sample volumes bloating and density reduction, so that the conductivity decreases.

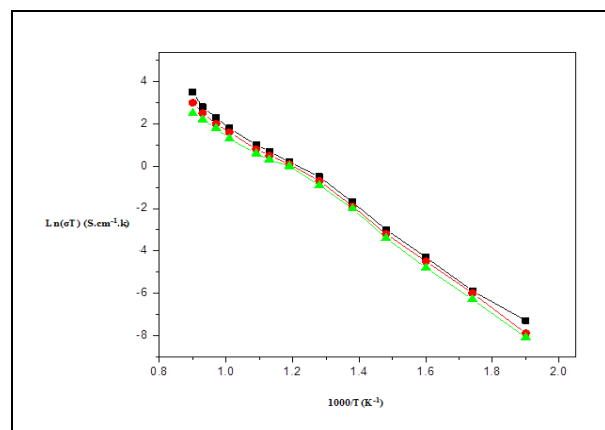


Fig. 6: Arrhenius plots for the Gd<sub>1-x</sub>Sr<sub>x</sub>AlO<sub>3</sub> of conductivity study.

#### 5. CONCLUSION

The present investigation was carried out to improve the performance of Gd<sub>1-x</sub>Sr<sub>x</sub>AlO<sub>3</sub> by the synthesis method. The electrochemical behavior of Gd<sub>1-x</sub>Sr<sub>x</sub>AlO<sub>3</sub> based on the method of synthesis and sintering temperature. The present work was mainly focused on synthesis, and ionic conductivity of Gd<sub>1-x</sub>Sr<sub>x</sub>AlO<sub>3</sub>.

#### FUNDING

This research received no specific grant from any funding agency in the public, commercial, or not-for-profit sectors.

#### CONFLICTS OF INTEREST

The authors declare that there is no conflict of interest.

## COPYRIGHT

This article is an open access article distributed under the terms and conditions of the Creative Commons Attribution (CC-BY) license (<http://creativecommons.org/licenses/by/4.0/>).



## REFERENCES

- Cabouro, G., Caboche, G., Chevalier, S. and Piccardo, P., Opportunity of metallic interconnects for ITSOFC: Reactivity and electrical property, *J. Power Sources*, 156(1), 39-44(2006).  
<https://doi.org/10.1016/j.jpowsour.2005.08.039>
- Hui S, Roller J, Yick S, Zhang X, Dec`es-Petit C, Xie Y, Maric R, Ghosh D, A brief review of the ionic conductivity enhancement for selected oxide electrolytes, *J. Power Sources*, 172, 493-502(2007).
- Kirannala Laishram, Rekha Mann, Richa Sharma, Dinesh Bhardwaj, Suman Shakya, and Neelam Malhan, Nd: GGG Nanopowders by Microwave Gel Combustion Route and Sinterability studies, *Defence Science Journal*, 64(5), 490-494(2014).  
<https://doi.org/10.14429/dsj.64.5409>
- Manuel Gaudon, Elisabeth Djurado, Norbert H. Menzler, Morphology and sintering behaviour of yttria stabilised zirconia (8-YSZ) powders synthesised by spray pyrolysis *Ceramics International*, 30(8), 2295-2303(2004).  
<https://doi.org/10.1016/j.ceramint.2004.01.010>
- Massoud Kahlaoui, Sami Chifi, Abdelwahab Inoubla, Adel Madani, Chaabane Chefi, Synthesis and electrical properties of co-doping with La<sup>3+</sup>, Nd<sup>3+</sup>, Y<sup>3+</sup>, and Eu<sup>3+</sup>-citric acid-nitrate prepared samarium-doped ceria ceramics, *Ceramics International*, 39(4), 3873-3879(2013).  
<https://doi.org/10.1016/j.ceramint.2012.10.230>
- Orera, A. and Slater, P. R., New chemical Systems for Solid Oxide Fuel Cells, *Chem. Mater.*, 22(3), 675-690(2010).  
<https://doi.org/10.1021/cm902687z>
- Rajasekhar, M., Subramania, A. and Muzhumathai, S., Microwave Synthesis of Nd<sub>1-x</sub>Ca<sub>x</sub>CoO<sub>3</sub> Nanopowders as Cathode Material for Intermediate Temperature Solid Oxide Fuel Cells, *European J. Appl. Sci. Technol.*, 1(2), 50-56(2014).
- Simeonovl, S., Kozhukharov, S., Grenier, J-C., Machkova, M. and Kozhukharov. V., Assessment of Nd<sub>2-x</sub>Sr<sub>x</sub>NiO<sub>4-d</sub> as a cathodic material for solid oxide fuel cell applications, *Journal of chemical technology and metallurgy*, 48(1), 104-110(2013).
- Singanahally, T., Aruna, Alexander, S., Mukasyan, Combustion synthesis and nanomaterials, *Current Option in Solid State and Materials Science*, 12(3-4), 44-50(2008).  
<https://doi.org/10.1016/j.cossms.2008.12.002>